North Carolina State University
Department of Nuclear Engineering

MOOSE Project

On

NE – 533 Nuclear Fuel Performance

Title:

Analysis of Nuclear Fuel Using MOOSE

By

Ogechukwu Joy Ozoani

Course Instructor: Dr Benjamin Beeler

February, 2025.

1. Introduction

This report details the numerical modeling of heat conduction in a cylindrical nuclear fuel pellet using MOOSE (Multiphysics Object Oriented Simulation Environment). The problem is formulated in a 2D RZ coordinate system and solved for both steady-state and transient conditions with constant and temperature-dependent thermal conductivity. Analytical solutions are used for comparison with the steady state numerical results. The peak temperature values were shown for the transient part.

Part 1 (with corrections)

2. Problem Description

The fuel pellet geometry Fig.1. consists of:

Fuel region: Radius = 0.5 cm

Gap region: Thickness = 0.005 cm

Cladding region: Thickness = 0.1 cm

Height: 1 cm

Outer cladding temperature: 550 K

Linear Heat Rate (LHR):

- Steady state: 350 W/cm
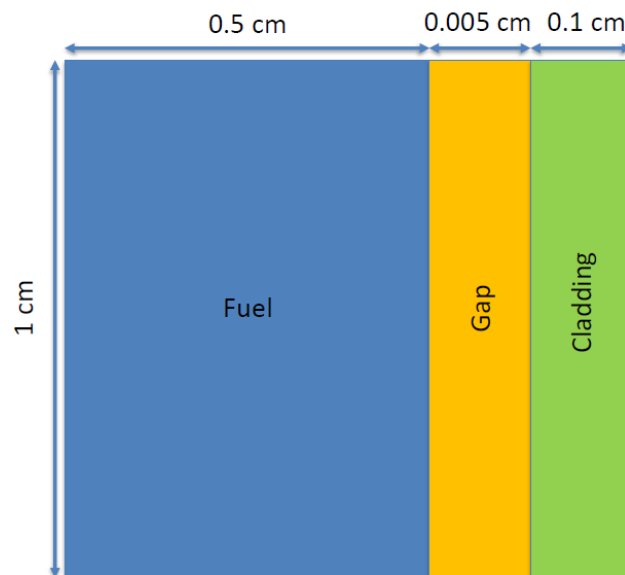- Transient: $350 \times \exp(-((t - 20)^2) \div 2) + 350$

Fig.1. Problem Definition and Geometry

3. Simulation Setup

3.1. Materials selection

The materials selected for the simulation for both steady state and transient with constant thermal conductivity represent typical components of a nuclear fuel rod:

- Fuel: Thermal conductivity of 0.03 W/cm-K, typical for uranium dioxide (UO_2) at operating conditions. [1]
- Gap: Filled with helium gas, having a thermal conductivity of 0.02334 W/cm-K [1]
- Cladding: Made of zirconium alloy, with a thermal conductivity of 0.17 W/cm-K, providing structural integrity and efficient heat dissipation. [1]

The materials selected for the simulation for both steady state and transient with temperature-dependent thermal conductivity, k_{th} (T) were:

- Fuel: Fink Model was considered given that MOOSE uses this model for UO2Thermal type [1] , [3]

The Fink equation: $kth_{95} = (\frac{100}{7.5408+17.692T_n+3.6142T_n} + \left(\frac{6400}{T_n^{5/2}}\right) \exp\left(-\frac{16.35}{T_n}\right))$

Where $T_n = \frac{T}{1000}$ which means Tn is the temperature in K divided by 1000 (Explanation of equation link)

$$kth = kth_{95}\left(\frac{1}{1-(2.6-0.5T_n)0.05}\right) = 0.0616 W/cm-K$$

- Gap: For pure He: $k_{gap} = 16x10^\wedge-6 * T^\wedge 0.79$ [1]
- Cladding: Thermal conductivity for zircaloy T range in K $298 \leq T < 1800$ [4]

$$kth(T) = A0 + A1 \times \left(\frac{T}{1000}\right) + A2 \times (\frac{T}{1000})^2 = 0.1519 W/cm-K$$

Where A0 = 12.767; A1 = -0.54348; A2 = 8.9818 are constants

3.2. Mesh selection

The mesh is structured as a 2D radial-axial model in rz coordinates, consisting of:

- A structured mesh with 660 radial elements and 1 axial element (QUAD4)
- Three subdomains: fuel, gap, and cladding

The resolution ensures a fine enough discretization to capture temperature gradients.

Mesh Convergence Study

A mesh convergence study was performed to ensure the solution is independent of mesh size while maintaining numerical stability. The radial mesh density (nx) was varied, and the maximum fuel temperature was recorded for each case.

Results and Observations

Table 1 – Record of the maximum fuel temperature at varied radial mesh density (nx)

Number of Elements (nx)	Max Temperature (K)	Convergence Status
0 - 100	**Failed**	**Not Converged**
330	1714.70	**Converged**
660	**1796.79**	**Converged (Optimal)**
1320	1777.18	Converged
2240	1782.50	Converged
5600	1784.32	Converged
11200	**Failed**	**Not Converged**

Key Findings:

- Meshes below nx = 100 failed to converge, meaning they were too coarse to capture physics properly.
- nx = 330 converges, but it underpredicts the max temperature.
- nx = 660 stabilizes the solution, making it the best trade-off between accuracy and efficiency.
- Refining the mesh beyond nx = 660 (e.g., nx = 1320, 2240, 5600) only results in minor temperature variations, confirming mesh independence.
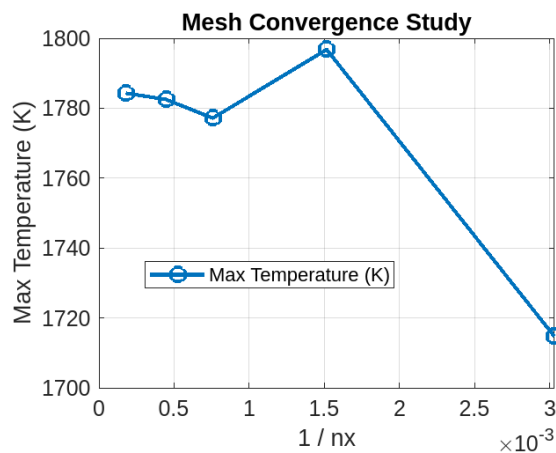- nx = 11200 leads to numerical instability, causing non-convergence.

Fig.2. Max temperature vs. inverse mesh size (1/nx)

This figure confirms that **nx = 660 is the optimal mesh**, as the solution stabilizes beyond this point.

Final Justification for Mesh Choice

- Meshes below nx = 100 fail to converge due to insufficient resolution.
- nx = 330 is stable, but it underpredicts the max temperature.
- nx = 660 is the optimal choice, as further refinement does not significantly change results.
- nx > 660 only results in minor temperature differences, confirming mesh independence.
- nx = 11200 causes numerical instability, making it impractical.

Based on this study, nx = 660 was selected as the optimal mesh resolution, ensuring accuracy, stability, and computational efficiency.

3.3. Variables

Temperature was defined. First-order elements were used for temperature interpolation. And Lagrange finite element family was used and since it uses nodal basis functions, the temperature was interpolated at the element nodes.

3.4. Kernels

ADHeatConduction type was used for both steady state and transient. It implements Fourier's law for heat conduction, ensuring temperature diffusion is modeled correctly:

$$\nabla \cdot (k \nabla T) = Q$$

The kernel consists of heat source block with type HeatSource which represents an external heat source term. This ensures localized heating in the fuel block.

ADHeatConductionTimeDerivative was considered since it represents the transient behavior of temperature, accounting for heat accumulation over time. The governing equation includes a time-dependent term:

$$\rho_{cp} = \frac{\partial t}{\partial T} = \nabla \cdot (k \nabla T) + q$$

3.5. Boundary and Initial Conditions

- Initial Temperature: 550 K (applied to the entire domain).
- Neumann BC at centerline (left boundary): Zero heat flux, ensuring symmetry.
- Dirichlet BC at outer cladding (right boundary): Fixed at 550 K, representing the outer cladding temperature.

Post-processors were implemented to extract the centerline temperature. The Newton solve-type was used to execute because it utilizes the Newton-Raphson method for solving nonlinear equations. Finally, CSV type was considered to generate output in CSV format

4. Results and Discussion

The simulation was run in MOOSE, and the temperature distribution was visualized using Paraview. The graphical results were generated using MATLAB.

4.1. Steady-state with constant thermal conductivity and steady-state with temperature-dependent thermal conductivity

The steady-state temperature distribution was obtained using MOOSE under two different thermal conductivity assumptions: constant and temperature-dependent thermal conductivity.
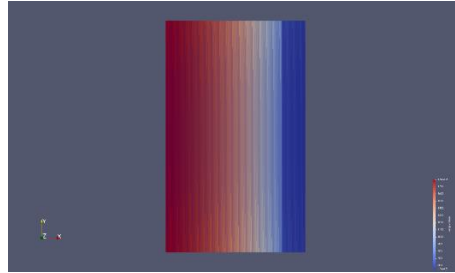
Visualization:

Fig.3. 2D image of steady state with constant kth

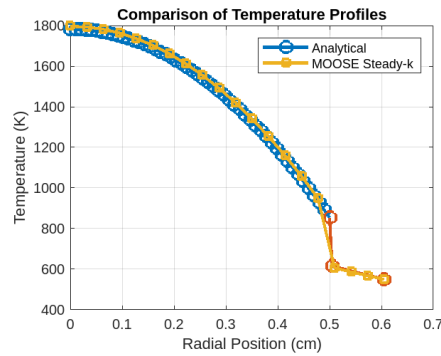**Comparison with Analytical Solution:**

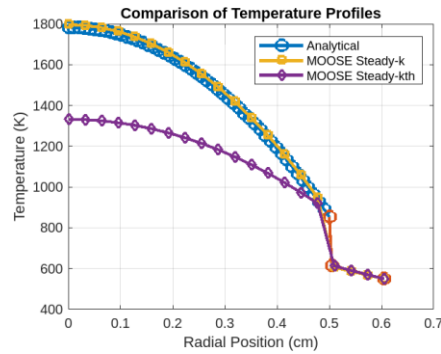Fig.4. Analytical solution vs steady state with constant kth

Fig.5. Analytical solution vs steady state with constant kth vs steady state with temperature-dependent kth

Key Observations:

- The maximum temperature is at the fuel centerline.
- A significant temperature drop occurs across the gap region.
- Outer cladding temperature is held at 550 K as per the boundary condition.

For constant thermal conductivity, MOOSE predicted a fuel centerline temperature of 1796.79 K, while the analytical solution gave 1782.11 K, with a minor 0.8% difference (14.68 K), mainly due to numerical discretization and boundary condition handling differences. This is shown in Fig. 4. When thermal conductivity was temperature-dependent, the centerline temperature decreased due to increased conductivity at higher temperatures, enhancing heat transfer. The comparison of steady-state centerline temperatures is shown in Fig. 5.

4.2. Transient with constant thermal conductivity and temperature-dependent thermal conductivity.
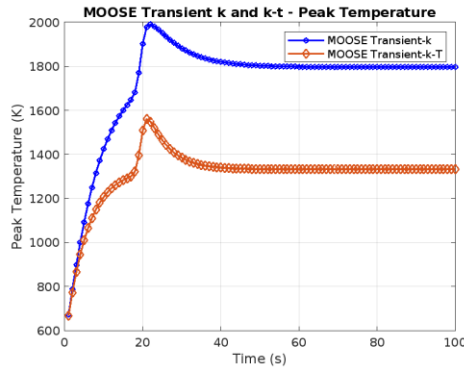
Temperature Evolution Over Time:

Fig.6. Transient with constant k vs transient with temperature-dependent kth

Peak Temperature values:

- **1989K** at 22nd time-step for transient with constant thermal conductivity.
- **1490K** at 24th time-step for transient with temperature dependent thermal conductivity.

Key Observation (Transient Case):

At the 100th time step, the fuel centerline temperature with constant thermal conductivity was 1796.13 K, closely matching the steady-state value of 1796.79 K, indicating near steady-state conditions in the transient simulation. For the temperature-dependent thermal conductivity case, the centerline temperature at the 100th step was 1332.10 K, consistent with the steady-state result for this model. The temperature drop compared to the constant conductivity case is due to higher thermal conductivity at elevated temperatures, improving heat dissipation and reducing the temperature gradient. This highlights the impact of temperature-dependent material properties on transient heat conduction, where the choice of conductivity model affects peak temperature predictions. Figure 6 shows the transient temperature evolution for both cases.

Part 2

5. Problem Description

- Fuel pin dimensions listed – 2D RZ. Figure 7.
- Assumption of reasonable values for thermal conductivities, T dependent
- Utilization of axial T_{cool}, with T_{cool_in} = 500 K, reasonable flow rate, heat capacity, etc.
- Utilization of axial LHR, with LHR^0 =350 W/cm
- Solve for the temperature profile for cladding surface, fuel surface, fuel centerline
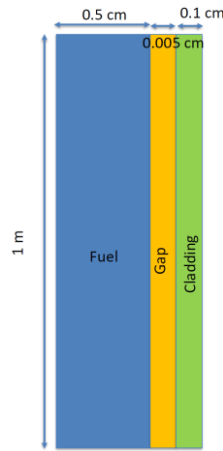- Determine the axial location of peak centerline temperature

Fig.7. Problem Definition and Geometry
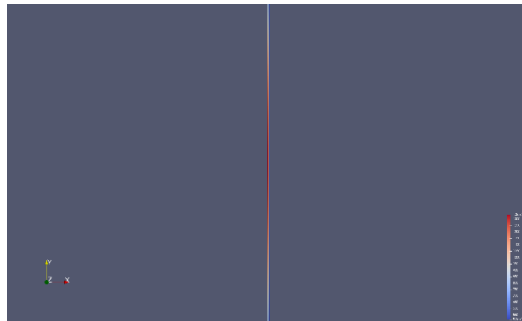
5.1. Results and Discussion

Fig.8. 2D image of steady state-kth showing the temperature axially

Observation: The temperature gradient is steepest near the centerline, which suggests that heat is being generated at the highest rate in the central portion of the fuel rod. The temperature drop towards the edges implies effective heat removal by the coolant flow.
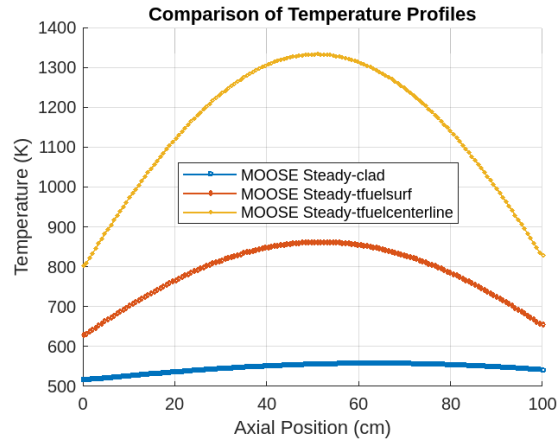
Fig.9. The temperature profile for the cladding surface, fuel surface and fuel centerline.

Observation: The plot shows symmetric steady-state temperature profiles, with peak values of around 557.219 K at 63.09 cm (cladding), 861.873 K at 51.68 cm (fuel surface), and 1332.77 K (fuel centerline) near the rod's midpoint at 51.01 cm. The large temperature gap between the cladding and fuel centerline indicates low fuel thermal conductivity. The gradual rise and fall in temperatures align with expected heat source and coolant effects, with the coolant maintaining the cladding temperature around 500–600 K.
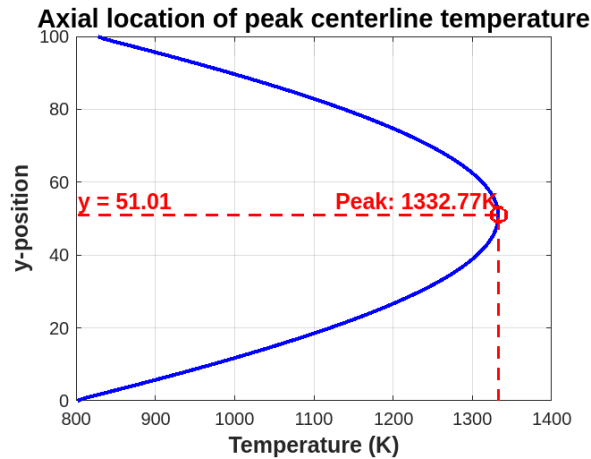

Fig.10. Axial location of peak fuel centerline temperature

Observation: The plot shows a symmetric temperature distribution along the y-position of the fuel rod, with a peak centerline temperature of 1332.77K at approximately 51.01 cm, matching the expected peak heat generation at the rod's midpoint. This reflects uniform heat generation and consistent coolant removal along the rod.
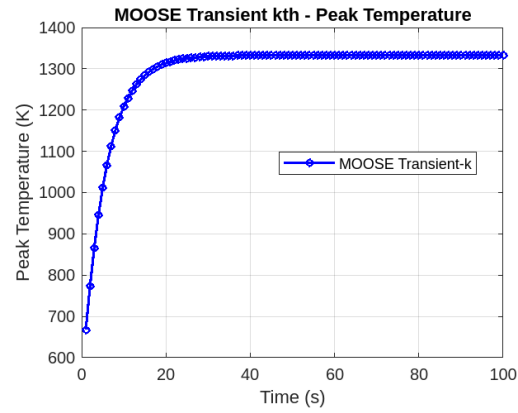
9

Fig.11. The peak centerline temperature for each time step at transient

Observation: The peak centerline temperature increases rapidly from 667.43 K to 1208.08 K during the first 10 time steps, then slows as it approaches steady-state conditions. By time step 40, the temperature reaches 1332.37 K, and by time step 60, it stabilizes at 1332.78 K, indicating near steady-state conditions. By time step 100, the temperature remains at 1332.79 K, confirming that the system has reached thermal equilibrium. The data shows a typical transient behavior with an initial rapid increase followed by gradual stabilization to a constant temperature.

6. Conclusion

This study analyzed the thermal behavior of a fuel rod under both steady-state and transient conditions, with a focus on temperature profiles at the cladding surface, fuel surface, and fuel centerline. The results showed that the temperature profiles under transient conditions mirrored those observed under steady-state conditions, with the peak centerline temperature reaching 1332.77 K at approximately 51.01 cm axially, which aligns with the maximum heat generation point in the rod. During the transient phase, the peak centerline temperature initially increased rapidly, reaching steady-state conditions by time step 60 and stabilizing at 1332.78 K. By time step 100, the temperature remained at 1332.79 K, confirming that the system had reached thermal equilibrium. These findings indicate that the transient response of the system closely follows the steady-state temperature profile, highlighting the importance of coolant flow and thermal conductivity in maintaining consistent thermal conditions.

7. References

[1] Nuclear fuel performance model 1 lecture 3 (slide 15, 26 and 31)

[2] J. K. Fink. Thermophysical properties of uranium dioxide. *Journal of Nuclear Materials*, 279(1):1–18, 2000. https://doi.org/10.1016/S0022-3115(99)00273-1

[3] Thermal conductivity empirical models in BISON to compute UO2 thermal conductivity and its dependence on temperature, porosity, burnup for UO2 fuel. (MOOSE FRAMEWORK)

[4] NASAGRC. Space Nuclear Propulsion Material Property Handbook Revision 000. Technical Report, National Aeronautics and Space Administration Glenn Research Center, Cleveland, Ohio, 2020.

[5] MOOSE (Homepage)